BNL-64953

Investigation of High-Energy-Proton Effects in Aluminum*

CONF-970201--

Carl J. Czajkowski, C. Lewis Snead, Jr., and Michael Todosow

Brookhaven National Laboratory

Upton, NY 11973-5000

USA

Abstract

Specimens of 1100 aluminum were exposed to several fluences of 23.5-GeV protons at the Brookhaven Alternating Gradient Synchrotron. Although this energy is above those currently being proposed for spallation-neutron applications, the results can be viewed as indicative of trends and other microstructural evolution with fluence that take place with high-energy proton exposures such as those associated with an increasing ratio of gas generation to dpa. TEM investigation showed significantly larger bubble size and lower density of bubbles compared with lower-energy proton results. Additional testing showed that the tensile strength increased with fluence as expected, but the microhardness decreased, a result for which an intepretation is still under investigation.

1100 Aluminum

Radiation will change the internal structure of many materials. In this research the effects of high-energy protons (23.5-GeV) on 1100 aluminum are emphasized. The effects of radiation on a material, of course, differ from general heating, in that radiation may localize large amounts of energy, whereas elevated temperatures will normally energize all of the atoms.

The primary processes of radiation damage in metals are transmutations and atomic displacements. Atomic displacements in a solid material can result in the alteration of many of its properties (e.g., increases in hardness and strength with concurrent decreases in toughness and ductility). Some of the earliest work [1] in this area considered this mechanism and subsequent gas production to be major contributors to mechanical-property changes.

Proton Irradiation

When the Department of Energy (DOE) initiated the New Production Reactors (NPR) Program to replace the aging defense production reactors, the use of a linear proton accelerator (for production of military-use tritium) was evaluated by the Energy Research Advisory Board (ERAB). ERAB concluded that an accelerator option, Accelerator Producer of Tritium (APT), could produce tritium. However, the amount of tritium then perceived as necessary would have required an APT accelerator needing 1000 MWe (mega-watts electric) for operation. It was concluded (by ERAB) that such a power requirement would push the operating cost into a noncompetitive region.

In November 1991, the Secretary of Energy decided that APT would be reevaluated. This evaluation was accomplished in January 1992 by the Jason panel, a DOE assigned senior consultant group. This group concluded that the APT option was technically feasible and could meet the demands of the projected new (lower) goal quantity of tritium.

In April 1992, the Secretary of Energy directed that a development program be initiated for the APT concept to support the record of decision (ROD) (a record of decision is the date at which one or two of the various tritium production methods will be selected for construction). The performance of these conceptual designs is to be determined through analysis and limited confirmatory experiments to characterize the production performance, the environmental impact, and safety of an accelerator facility.

The materials effort directed by this program included evaluating possible alloys for use in a 1-GeV proton beam to an anticipated 1.7×10^{23} p/cm^2 for target/window life. This value ($\sim 1.7 \times 10^{23}$ p/cm^2) was used as a base line projection for one year's operation of a window in the APT beam.

Aluminum alloys [2, 3, 4, 5, 6,] are the first choice as structural materials for the APT primarily due to their favorable low thermal neutron absorption cross section. Aluminum alloys have been in use on accelerators and have a much faster radioactivity decay (than stainless) leading to lower ALARA (As Low As Reasonably Achievable) human exposure considerations

during maintenance operations. Note: aluminum alloys decay approximately five times faster than stainless steels. It was necessary to verify the integrity of the alloys already in use in the accelerator and reactor communities to assure the safety of the present design.

The materials test program consisted of evaluation and characterization of previously-proton-irradiated window/target materials. Evidence of materials degradation through either microstructural or mechanical-property deterioration were to be investigated and evaluated. Comparison to archive specimen mechanical/microstructural properties were performed wherever possible. The material tested/evaluated and reported here is: Aluminum alloy 1100, proton irradiated in the BNL Alternating Gradient Synchrotron (AGS) at 23.5 GeV to a fluence of ~10^{18} p/cm^2. Unirradiated archival material was also evaluated. Tensile tests were performed on the procured archival stock materials. Additionally, microhardness measurements were made on the 1100 aluminum. Microhardness measurements were performed since the irradiated materials were in the form of thin sheets and this method of testing would ensure consistency of measured data. Table 1 lists the results of the tensile tests performed on the archival stock.

Table 1

1100 Aluminum Mechanical Properties

Specimen Number (a), Displacement at Peak (mm) (b), % Strain at Peak (%) (c), Load at Peak (kg) (d), Stress at Peak (Mpa) (e), Stress at 0.2% Yield (Mpa) (f), % Strain at Break (%) (g), Stress at Break (Mpa) (h)

a	b	c	d	e	f	g	h
1	3.05	12.00	209.3	104.0	44.5	19.30	46.5
2	2.73	10.76	209.7	104.1	43.2	18.76	65.1
3	2.53	9.98	209.	103.8	40.5	21.88	6.9
Mean	2.8	10.91	209.4	104.0	42.7	19.98	39.5
Standard Deviation	0.26	1.02	0.32	0.02	2.1	1.67	29.7

The microhardness data for the archival materials is tabulated in Table 2. Two sets of microhardness values were recorded for each material. This was done to determine if one of the two methods of transmission electron microscope (TEM) specimen cutting imparted work hardening to the material. The questionable method of specimen cutting involved a punch, which could cut a 3-mm diameter specimen. The second method of TEM specimen cutting utilized electric discharge machining (EDM). EDM is a process in which the work piece is machined or eroded by electrical energy of high density. In EDM, machining spark erosion takes place in a nonconducting or dielectric fluid. The work piece and EDM electrode are submerged in the dielectric, which is usually oil. The dielectric fluid concentrates the arc energy and flushes away the material eroded from the work piece. Although no work- hardening effects on the specimens cut by either of these methods were observed, it was determined that EDM would be used, whenever possible, for ALARA considerations.

Table 2

1100 Aluminum Microhardness Test Results (KN)

EDM	Punch
47,43,43,43,43,44 Avg. 44 KN	43,43,44,43,43 Avg. 43 KN

Electron Microscopy

Scanning Electron Microscopy (SEM)

The fracture faces of each of the materials tensile tested were examined by SEM. This evaluation was used to evaluate the mode of fracture from the uniaxial tensile pulls. Figure 1 is the low magnification fracture surface associated with the 1100 aluminum. The fracture was of the dimpled rupture type (Figure 2) which is typical of a ductile material failure. These dimples

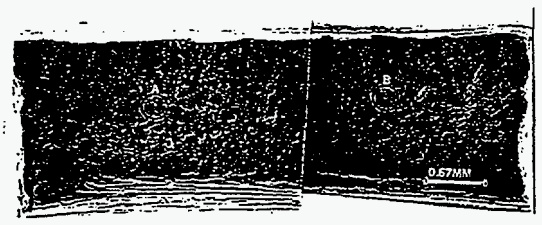

Figure 1. Low- magnification SEM photograph of the resultant fracture from a tensile failure in 1100 Al. Areas a and B are locations of high-magnification fractographs.

DISCLAIMER

Figure 2. Dimpled ruptured appearance was seen in Area A.

are depressions in the microstructure and occur by a process of microvoid nucleation in areas of high plastic strain. Various metallic inhomogeneities are preferred sites for this microvoid nucleation, e.g., inclusions, precipitates, grain boundaries. As the strain increases, these microvoids expand and finally rupture producing the dimpled rupture appearance [7].

Transmission Electron Microscopy (TEM)

A number of unirradiated test specimens were thinned in order to develop the proper technique (thinning parameters) prior to use on the proton irradiated materials.

The etching solutions decided upon for this project were:

A. Methyl-Nitric Electrolyte (3:1)
750 ml methanol
250 ml nitric acid (conc.)
Thinned at: ~-25°C, 15 volts, 140-160m A

After thinning, the various specimens were stored in partitioned boxes and placed in designated and identified containers. The specimens were then examined by TEM.

The 1100 aluminum material was examined by electron microscopy. The 1100 alloy, which is 99.2% pure aluminum, had dislocations present. The 1100 material (Figure 3) had subcell dislocation networks associated with the grains. The major impurities identified were Si and Fe.

Figure 3. TEM photo showing a subcell dislocation network in 1100 Al.

Proton Irradiation of 1100 aluminum at the Alternating Gradient Synchrotron (AGS)

The opportunity to irradiate some samples of 1100 aluminum in the AGS arose. The proton energy of these irradiations was approximately 23.5 GeV. A total of 24 - 15x15-cm sheets of 0.050-cm-thick 1100 aluminum were placed in a beam hall of AGS.

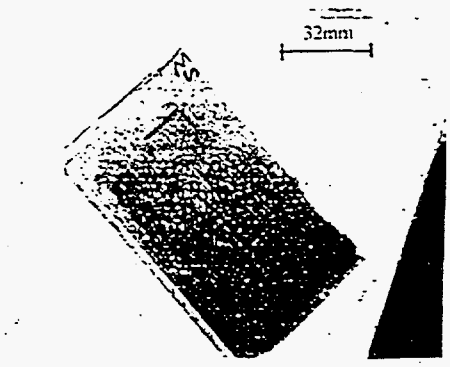

Figure 4. Photograph of tensile/TEM microhardness specimen layout.

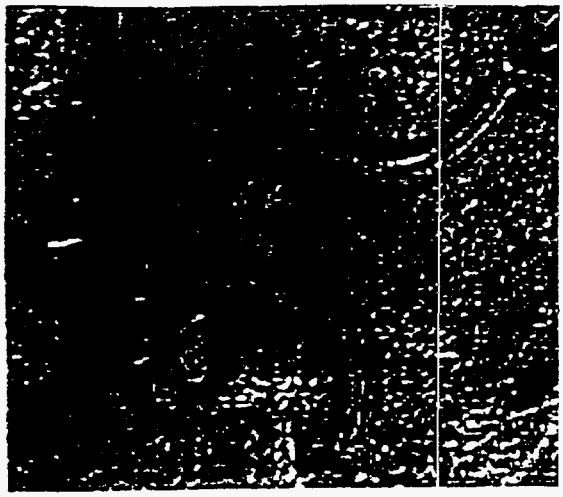

Figure 5. Close-up photo showing specimen location (typical).

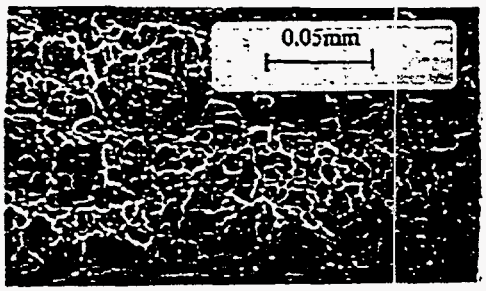

Figure 6. Low-magnification fractograph showing ductile fracture face after tensile test (typical).

After irradiation, the area of maximum proton fluence was determined using a photographic film technique. This area (of highest fluence) had tensile, microhardness, and TEM specimens cut from it. Figure 4 is a photograph of the 15-cm square disk in the electric-discharge machining (EDM) unit. Figure 5 provides a closeup of the specimen location on the aluminum sheet.

Table 3

Microhardness and Tensile Test Results on 1100 Aluminum
AGS Run (23.5 GeV, 10^{18}p/cm^2)

Specimen	Irradiated/ Unirradiated	Tensile Str (Mpa)	Hardness KN (Avg. of 5)
1	Un	100.2	44
2	Un	100.7	44
3	Un	100.7	44
4	Irr	103.4	35.66
5	Irr	104.5	31.9
6	Irr	105.0	32.04
7	Irr	101.3	31.42

The smaller (circular) specimens were cut to provide: 1 microhardness specimen; 1 TEM specimen, and 2 archive specimens. The large "dog bone" style specimen was the tensile specimen. Figure 6 is a fractograph of a typical tensile test specimen tested (3 total), which showed a desirable "dimpled rupture" (ductile) fracture. Table 3 lists the results of the tensile and microhardness measurements taken.

It can be seen that there was a reduction in hardness in the material (44 KN to 32.75 KN). This would normally indicate a reduction in tensile strength. This was not the case as the tensile strength appeared to increase approximately (1-2)%, which is within the scatter band of the tensile test (using 1 specimen/test). Note: Knoop microhardness values are determined by measuring the size of the unrecovered indentation and comparing this value to formulas or tables meeting established standards. The Knoop indenter "... is a highly polished, rhombic-based pyramidal diamond that produces a diamond-shaped indentation with a ratio between long and short diagonals of about 7 to 1."

The Knoop indenter produces a depth of indentation approximately one-thirtieth its length. The developed Knoop hardness number (HK) is equal to the ratio of the applied load to the unrecovered projected area:

$$HK = P/A = P/CL^2 \qquad (1)$$

where:

P = applied load
A = unrecovered projected area of indentation
L = measured length of long diagonal
C = constant for indenter relating area of indentation to the square of the long diagonal.

Figure 7 is a representation of the load versus hardness combinations for determining minimum thicknesses of sheet that can be tested. The 100-g loadings used for these experiments adequately covered the range of material thicknesses examined (0.127 mm - 0.508 mm). TEM photographs of the 1100 aluminum irradiated with 23.5-GeV protons showed no microstructural changes in the metal, but definite areas of cavity formation (Figures 8-9).

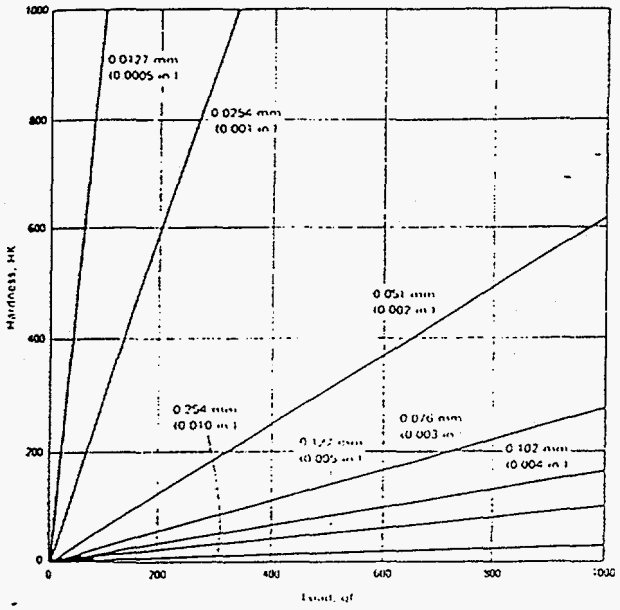

Figure 7. Knoop minimun-thickness chart. Indicates load and hardness combinations for determining the minimum thickness of sheet or foil that can be tested.

Figure 8. Cavities were visible in the 1100 Al irradiated by 23.5-GeV protons (58,000X).

Figure 9. Formation of cavities at a grain boundary occurred in this area of 1100 Al irradiated by 23.5-GeV protons (190,000X).

Discussion

The TEM results indicate that the 1100 aluminum did not undergo significant microstructural changes after irradiation by 23.5-GeV protons. It appears that it is the fluence of protons which will affect the mechanical properties for the application, not necessarily the energy level of the protons. The microstructural examination (TEM) did not disclose additional damage mechanisms, other than those previously observed [5, 6, 8, 9, 10, 11, 12] at differing energies. Therefore, the type of damage to the material was caused by the fluence of protons impacting the specimen, not necessarily the energy level of the protons.

The 1100 aluminum which had been irradiated with 23.5-GeV protons increased in tensile strength. This increase in tensile strength is expected due to the previously described displacement hardening mechanism. The reduction in microhardness values from an average value of 44 KN (irradiated) to an average value of 32.75 KN (unirradiated) cannot easily be interpreted. (NOTE: No instrumentation was available for temperature measurements during these irradiations). One possible explanation involves the areas of cavity formation seen in the TEM studies. Previous studies [12] of gas accumulation in aluminum after 800-MeV proton irradiations indicated that higher-energy proton irradiations (800-MeV versus 600-MeV) form larger bubbles in the irradiated materials. This increase in bubble size was accompanied by a significant decrease in bubble density (~30 to 1) with increasing proton energy. There were no references available in the literature with information on proton irradiations in the 1.0+ GeV range, so only suppositions at this point are available until additional data are developed. It should be kept in mind,

however, that cavity size and growth can be affected by gas generated by the spallation process, and that the number of gas atoms generated per dpa increases almost linearly with proton energy in the Gev range.

If one follows the logic that the greater the increase in energy, the larger the cavities formed in the MeV ranges, then the GeV energies could produce large enough cavities actually to affect microhardness measurements. Pyramid indenter anomalies have been observed [8] in annealed metals when a sinking in of the metal around the flat faces of the pyramid results in overestimating the hardness of the work piece. The use of an ultrasonic hardness testing system (if sufficiently sensitive) would effectively eliminate the effects of internal gas cavities, and might be effective in determining if microhardness measurements are affected by gas bubble density in the 1100 aluminum. Without question, additional work is needed in the GeV range of energies to resolve this apparent contradiction between the tensile strength and microhardness measurements; and will be investigated if additional beam time in the AGS becomes available.

Acknowledgments

* This work was performed under the auspices of the U. S. Department of Energy under Contract No. DE-AC02-76CH00016.

References

1. Greenwood, G.W., Foreman, A.J.E., and Rimmer, D.E., "The Role of Vacancies and Dislocations in the Nucleation and Growth of Gas Bubbles in Irradiated Fissile Material", J.of Nuclear Materials, 4 (1959), 305-324.

2. Wechsler, M.S., Stubbins, J.F., Sommer, W.F., Ferguson, P.D., and Farnum, E.H., "Selection and Qualification of Materials for the Transmutation of Waste Project", Los Alamos Report, LA-UR-92-1211, 1992.

3. Graber, M.J., and Ransick, J.H., "ETR Damage Surveillance Programs, Progress Report 1", January 27, 1961.

4. Singh, B.N., Lohmann, W., Ribbens, A., and Sommer, W.F., "Microstructural Changes in Commercial Aluminum Alloys Caused by Irradiation with 800-MeV Protons", ASTM STP 955, Radiation Induced Changes in Microstructure: 13th International Symposium (Part 1), 1987, 508-519.

5. Lohmann, W., Ribbens, A., Sommer, W.F., and Singh, B.N., "Microstructure and Mechanical Properties of Medium Energy (600-800 MeV) Proton Irradiated Commercial Aluminum Alloys", Radiation Effects, 1986, Vol. 101, 283-299.

6. Singh, B.N., Lohmann, W., Ribbens, A., and Sommer, W.F., "Microstructural Changes in Commercial Aluminum Alloys Caused by Irradiation with 800-MeV Protons", ASTM STP 955, Radiation-Induced Changes in Microstructure: 13th International Symposium, 1987, 508-519.

7. An Atlas of metal Damage, Engel, L. and Klingle, H., Prentice-Hall, Inc., 1981.

8. Metals Handbook, Ninth Edition, Volume 8, Mechanical Testing, American Society for Metals, Metals Park, OH 44703 (1985).

9. Victoria, M., Green, W.V., Singh, B.N., and Leffers, T., "Nucleation, Growth, and Distribution of Cavities in the Vicinity of Grain Boundaries in Aluminum Irradiated with 600-MeV Protons", ASTM STP 955, Radiation-Induced Changes in Microstructure: 13th International Symposium, 1987, 233-241.

10. Paschoud, F., Gotthardt, R., and Green, S.L., "Stability Studies of Radiation Defects in Aluminum Introduced by 600-MeV Protons", ASTM STP 955, Radiation-Induced Changes in Microstructure: 13th International Symposium, 1987, 478-489.

11. Gavillet, D., Green, W.V., Victoria, M., Gotthardt, R., and Martin, J-L., "In-Situ Electron Microscopy Observation of Dislocation Motion in 600-MeV Proton Irradiated Aluminum", ASTM STP 955, Radiation-Induced Changes in Microstructure: 13th International Symposium, 1987, 490-497.

12. Singh, B.B., Horsewell, A., Sommer, W.F., and Lohmann, W., "Gas Accumulation at Grain Boundaries During 800-MeV Proton Irradiation of Aluminum and Aluminum Alloys", J. Of Nuclear Materials, 141-143, 1986, 718-722.